Magnetic properties of the triangular-lattice multilayer antiferromagnet with single-site anisotropy

2000 J. Phys.: Condens. Matter 12 2819

(http://iopscience.iop.org/0953-8984/12/12/320)

J. Phys.: Condens. Matter **12** (2000) 2819–2824. Printed in the UK PII: S0953-8984(00)05926-9

Magnetic properties of the triangular-lattice multilayer antiferromagnet with single-site anisotropy

Zhan-Hai Dong†‡§‖ and Shi-Wei Gu‡

† Minhang Campus A9807092, Shanghai Jiao Tong University, Shanghai 200240, People's Republic of China
‡ Department of Applied Physics, Shanghai Jiao Tong University, Shanghai 200240, People's Republic of China
§ Yanbei Teachers' College, Dating 037000, People's Republic of China

Received 12 July 1999, in final form 6 January 2000

Abstract. The Heisenberg antiferromagnet with single-site anisotropy on the fully frustrated multilayer triangular lattice is investigated by employing the double-time Green's function. The origin of the spin gap is analysed; it is suggested to be closely related to the magnetic anisotropy. The axial and planar susceptibilities and the specific heat are calculated. The theoretical result agrees with that of a Monte Carlo simulation and that of an experiment on the compounds $CsMnI_3$ and $CsMnBr_3$.

Recent years have seen a flurry of interest caused by the triangular-lattice Heisenberg antiferromagnets (THAF) [1–4]. The attention is attracted mainly because of the fully frustrated system having spin-glass-like disordered ground states and relates to high-temperature superconductivity. It is known that the high-T_c superconductors are highly anisotropic, and have layered structure with strong intra-planar and weak inter-planar coupling. Some efforts have been made to research the properties of the inter-planar coupling systems [3, 5]. Furthermore, the single-site anisotropy in layered-structure materials has also motivated some authors' interest [6] because single-site anisotropy is crucial to the phase transitions and the critical behaviour of some magnets, for example the compounds $CsMnI_3$ and $CsMnBr_3$ [7].

Here our attention is focused on the triangular-lattice multilayer Heisenberg antiferromagnet with single-site anisotropy without long-range order (LRO). The magnet consists of multiple layers of triangular lattice, one on top of another, with the intra-planar spin coupling parameter $J_{ab} = 1$, the inter-planar parameter $\rho = J_c/J_{ab}$, and the single-site anisotropy $\lambda = J_d/J_{ab}$. The standard HAF Hamiltonian is expressed as

$$H = \sum_{\langle ij \rangle} \boldsymbol{s}_i \cdot \boldsymbol{s}_j + \rho \sum_{\langle lm \rangle} \boldsymbol{s}_l \cdot \boldsymbol{s}_m - \lambda \sum_i (s_i^z)^2 \tag{1}$$

where the first and second terms are the intra- and the inter-plane couplings, respectively. The last term denotes the single-site anisotropy. In order to compare the theoretical results with those from the experiments, the quantity ρ is fixed at 0.2, and the spin of the magnet is supposed to be $S = 5/2$. However, λ is varied to allow one to investigate the behaviour of the single-site anisotropy.

‖ Author to whom any correspondence should be addressed.

0953-8984/00/122819+06$30.00

If the single-site anisotropy term $\lambda \sum_i (s_i^z)^2$ is dropped, the Hamiltonian retains rotational symmetry; consequently the planar correlation function $\langle s_i^\alpha s_j^\alpha \rangle$ ($\alpha = \langle x, y \rangle$) equals the axial one $\langle s_i^z s_j^z \rangle$, and in double-time Green function theory only one Green function is introduced [5]. However, the single-site anisotropy destroys the rotational symmetry, i.e., the planar correlation function differs from the axial one. In this case two Green functions $\langle\langle s_i^\dagger; s_j^- \rangle\rangle$ and $\langle\langle s_i^z; s_j^z \rangle\rangle$ must be introduced, and their time Fourier transforms $G(n, \omega) = \langle\langle s_i^\dagger; s_{i+n}^- \rangle\rangle$ and $G_z(n, \omega) = \langle\langle s_i^z; s_{i+n}^z \rangle\rangle$ satisfy the equation of motion

$$\omega \langle\langle A; B \rangle\rangle = \frac{1}{2\pi} \langle [A, B] \rangle + \langle\langle [A, H]; B \rangle\rangle \tag{2}$$

where $[\cdot, \cdot]$ denotes the commutator, $\langle \cdots \rangle$ the thermal average, and $\langle\langle A; B \rangle\rangle$ the time Fourier transform of the Green function. Introducing order parameters $C_1 = \langle s_0^\dagger s_1^- \rangle$ and $D_1 = \langle s_0^z s_1^z \rangle$, and employing the Kondo–Yamaji Green function decoupling scheme [5,8], we can obtain the space Fourier transforms of the Green functions and correlation functions:

$$G_z(k, \omega) = -\frac{1}{2\pi} \frac{C_1(\Gamma_k + \rho\Gamma_{ck})}{\omega^2 - \omega_k^2} \tag{3}$$

$$G(k, \omega) = -\frac{1}{2\pi} \frac{(2D_1 + C_1)(\Gamma_k + \rho\Gamma_{ck}) - 2\lambda(2D_0 - C_0)}{\omega^2 - \Omega_k^2} \tag{4}$$

$$D_n = \langle s_0^z s_n^z \rangle = -\frac{1}{N} \sum_{\boldsymbol{k}} \mathrm{e}^{-\mathrm{i}\boldsymbol{k}\cdot\boldsymbol{n}} \frac{C_1(\Gamma_k + \rho\Gamma_{ck})}{2\omega_k} \coth\left[\frac{\omega_k}{2k_\mathrm{B}T}\right] \tag{5}$$

$$C_n = \langle s_0^\dagger s_n^- \rangle = -\frac{1}{N} \sum_{\boldsymbol{k}} \mathrm{e}^{-\mathrm{i}\boldsymbol{k}\cdot\boldsymbol{n}} \frac{(2D_1 + C_1)(\Gamma_k + \rho\Gamma_{ck}) - 2\lambda(2D_0 - C_0)}{2\Omega_k} \coth\left[\frac{\Omega_k}{2k_\mathrm{B}T}\right] \tag{6}$$

where

$$\Gamma_k = z(1 - \gamma_k) \qquad \Gamma_{ck} = z_c(1 - \gamma_{ck})$$
$$\gamma_k = (1/z) \sum_{\boldsymbol{\eta}} \mathrm{e}^{-\mathrm{i}\boldsymbol{k}\cdot\boldsymbol{\eta}} \qquad \gamma_{ck} = (1/z_c) \sum_{\boldsymbol{\delta}} \mathrm{e}^{-\mathrm{i}\boldsymbol{k}\cdot\boldsymbol{\delta}}$$

with η and δ being the nearest-neighbour vectors in and out of the plane, respectively. The quantities z and z_c refer to the numbers of nearest-neighbour sites in and out of the plane, respectively, and k_B and $\boldsymbol{n}$ refer to the Boltzmann constant and the lattice vectors, respectively. The sum rule satisfies $C_0 + D_0 = \langle s_n^\dagger s_n^- \rangle + \langle s_n^z s_n^z \rangle = S(S + 1)$. The two branches of the spin-excitation spectra ω_k and Ω_k are

$$\begin{aligned}\omega_k^2 = {} & (C_0 + \alpha C_1)(\Gamma_k + \rho^2\Gamma_{ck}) + 2\alpha\lambda C_1(\Gamma_k + \rho\Gamma_{ck}) \\ & - [C_1 + 2(\alpha - 1)D_1][\Gamma_k(1 + z\gamma_k + z_c\rho\gamma_{ck}) + \rho\Gamma_{ck}(z\gamma_k + z_c\rho\gamma_{ck} + \rho)] \\ & + \xi_2\Gamma_k + \rho\xi_3(\Gamma_k + 3\Gamma_{ck}) + \rho^2\xi_4\Gamma_{ck}\end{aligned} \tag{7}$$

$$\begin{aligned}\Omega_k^2 = {} & \frac{1}{2}(C_0 + 2D_0)(\Gamma_k + \rho^2\Gamma_{ck}) - \frac{\alpha}{2}[(C_1 + 2D_1)(z\gamma_k + z_c\rho\gamma_{ck})(\Gamma_k + \rho\Gamma_{ck}) \\ & - (\xi_2' + \rho\xi_3')\Gamma_k - \rho(3\xi_3' + \rho\xi_4')\Gamma_{ck} - 2\lambda C_1(\Gamma_k + \rho\Gamma_{ck})] + \Delta_\lambda^2(k)\end{aligned} \tag{8}$$

where

$$\xi_l = C_l' + 2(\alpha - 1)D_l' \qquad \xi_l' = C_l' + 2D_l' \qquad (l \geqslant 2)$$

with C_l' and D_l' denoting

$$X_2' = \sum_{\eta' \neq \eta} X_{\eta - \eta'} \qquad X_3' = \sum_{\delta} X_{\eta - \delta} \qquad X_4' = \sum_{\delta' \neq \delta} X_{\delta - \delta'} \qquad (X = C, D).$$

The quantity α is the decoupling parameter introduced originally by Kondo and Yamaji [8], and the quantity $\Delta_\lambda(k)$ represents the spin-gap function:

$$\Delta_\lambda^2(k) = -2\alpha\lambda(C_1 + D_1)(\Gamma_k + \rho\Gamma_{ck}) + 4\lambda^2 D_0 + \alpha\lambda(z + z_c\rho)(C_1 - 2D_1) - \lambda(C_0 - 2D_0)(z\gamma_k + z_c\rho\gamma_{ck}). \tag{9}$$

Equations (5)–(8) constitute a self-consistent equation set which determines all the parameters introduced. In the isotropic case ($\lambda = 0$) the Hamiltonian has rotational symmetry and the correlation function satisfies $C_n = 2D_n$. With this in mind we can easily conclude that $G(k, \omega) = 2G_z(k, \omega)$ from equations (3) and (4), and that $\Omega_k = \omega_k$ from equations (7) and (8), which means that the theory is self-consistent. It is stressed that in the isotropic case the present spin-excitation spectrum cannot be reduced to the previous one [5] where the magnetic spin was supposed to be $1/2$. The reason for this is that the commutation relationship $s^z s^\sigma = \sigma s^\sigma/2$ ($\sigma = \pm 1$) holds for the case of $S = 1/2$ but does not hold for the case of $S > 1/2$.

Figures 1(a)–1(c) show the spin-excitation spectra in the cases of $\lambda = 0.02$, 0.2, 0.4, respectively. The solid line represents the acoustic branch with E_t denoting its band top. The dashed line represents the optical branch with E_b denoting its band bottom. For small $\lambda \approx 0.02$ we have $E_t > E_b$ (figure 1(a)) which means that the two branches overlap and the excitation is gapless. When λ reaches the critical value $\lambda_c \approx 0.2$ we have $E_t = E_b$ (figure 1(b)) which means that the excitation is still gapless. If the single-site anisotropy parameter λ exceeds λ_c we have $E_t < E_b$ which means that the spin gap starts to open. For large λ a large gap opens (figure 1(c)).

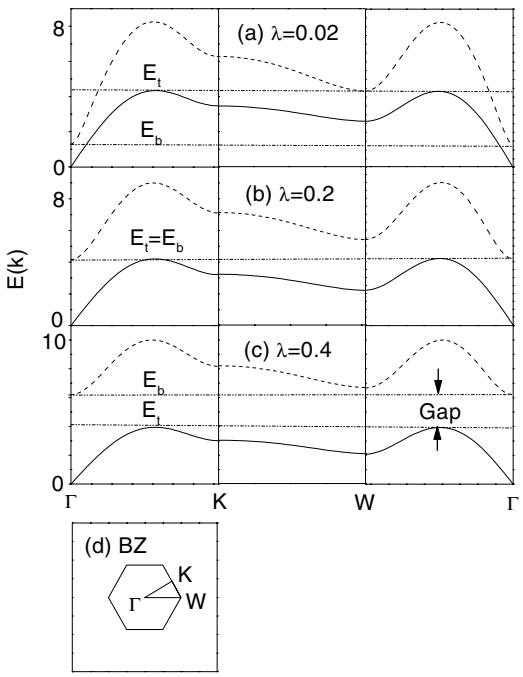

Figure 1. The acoustic and optical spin-excitation spectra $\omega(k)$ (solid line) and $\Omega(k)$ (dashed line) in the cases of (a) $\lambda = 0.02$, (b) $\lambda = \lambda_c \approx 0.2$, and (c) $\lambda = 0.4$. The quantity E_t (E_b) represents the band top (bottom) of the acoustic (optical) branch, and the straight dash–dotted lines are guides to the eye. The plot (d) represents the Brillouin zone.

The origin of the spin gap has attracted much attention. There are even opposite opinions about its physical mechanism. Some authors argued that the origin of the spin gap was not an intrinsic property of the planar spin dynamics but rather results from the antiferromagnetic coupling of layers [9]. Others believed it likely that the appearance of a spin gap was not related to the presence of layers but rather reflects a crossover in the spin dynamics from an overdamped to a quantum disordered regime [10]. In our opinion, the appearance of the spin gap may be related to magnetic anisotropies such as the Dzyaloshinski–Moriya interaction, the easy-axis-type and easy-planar-type anisotropies, and the above-discussed single-site anisotropy. Any anisotropy that breaks the rotational symmetry of the Hamiltonian may result in the spin excitation splitting into several branches. If this kind of anisotropy is large enough to separate the spin-excitation branches from each other, a spin gap opens.

In the case of $\lambda \neq 0$ the static magnetic susceptibility is also anisotropic, i.e., the axial component χ_{zz} (external field parallel to z-axis) differs from the planar component $\chi_{\alpha\alpha}$ (external field parallel to α-axis; $\alpha = \langle x, y \rangle$):

$$\chi_{zz} = \frac{g^2\mu_B^2}{k_B T} \sum_n D_n = -\frac{g^2\mu_B^2 (z + z_c\rho) C_1}{\omega_0^2} \tag{10}$$

$$\chi_{\alpha\alpha} = \frac{g^2\mu_B^2}{2k_B T} \sum_n C_n = \frac{\lambda g^2\mu_B^2}{k_B T} \frac{2D_0 - C_0}{\Delta_0} \coth\left[\frac{\Delta_0}{2k_B T}\right] \qquad (\lambda \neq 0) \tag{11}$$

where ω_0^2 is ω_k^2 when Γ_k is replaced with z, Γ_{ck} with z_c, γ_k and γ_{ck} with 1; Δ_0 is $\Delta_\lambda(k)$ when Γ_k and Γ_{ck} are replaced with zero, γ_k and γ_{ck} with 1.

Figures 2 and 3 show the susceptibilities χ_{zz} and $\chi_{\alpha\alpha}$ versus reduced temperature T/J_{ab}. The axial susceptibility χ_{zz} has a clear peak near $T \sim J_{ab}$, but the planar susceptibility $\chi_{\alpha\alpha}$

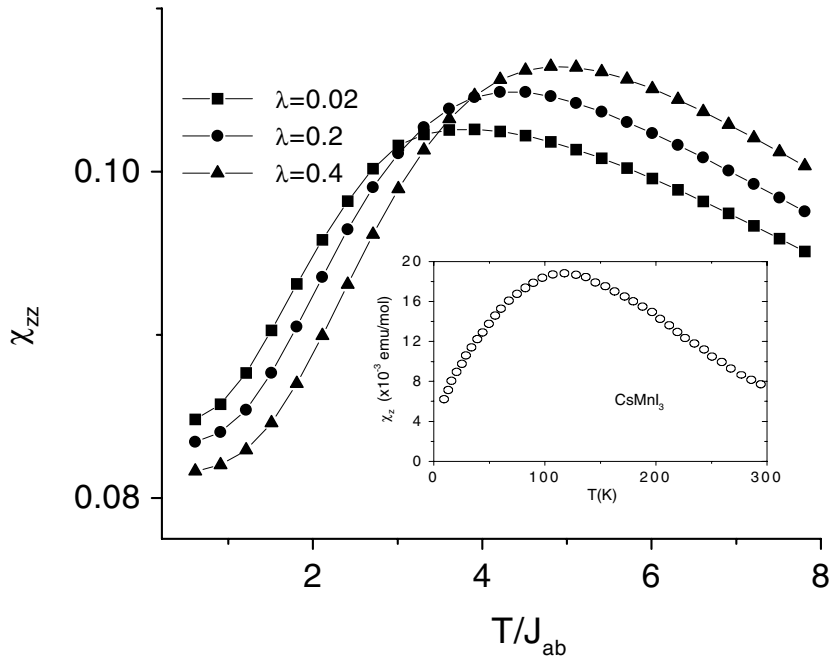

Figure 2. The axial susceptibility scaled with $(g\mu_B)^2$ versus the reduced temperature T/J_{ab} in the cases of $\lambda = 0.02$, 0.2, and 0.4. The inset represents the experimental results taken from reference [7].

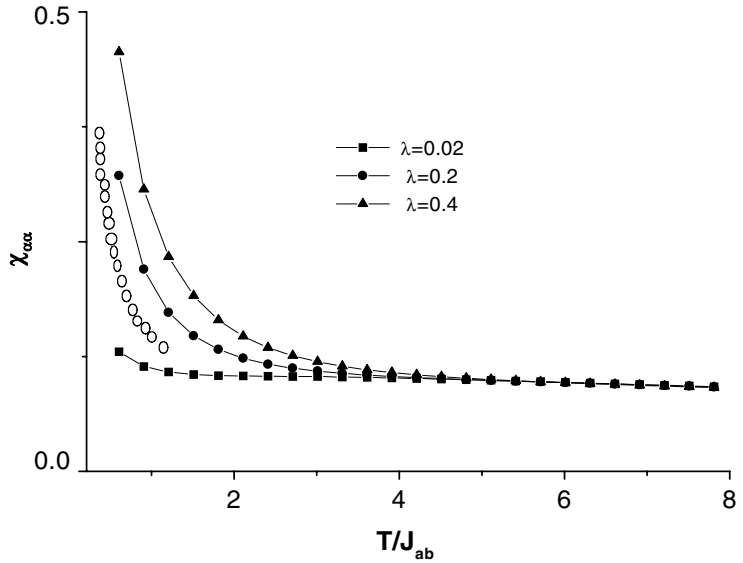

Figure 3. The planar susceptibility scaled with $(g\mu_B)^2$ versus the reduced temperature T/J_{ab} in the cases of $\lambda = 0.02, 0.2$, and 0.4. The line of circles represents the Monte Carlo simulation result taken from reference [6].

behaves quite differently and increases monotonically with the decreasing temperature. In particular, when the temperature approaches zero, $\chi_{\alpha\alpha}$ goes up abruptly. The highly anisotropic susceptibilities can be attributed to the appearance of the single-site anisotropy. The data on the axial susceptibility are in qualitative agreement with those from an experiment on the compounds $CsMnBr_3$ and $CsMnI_3$ [7]. For convenience of comparison, the experimental results are replotted as an inset in figure 2. The data on the planar susceptibility are in good agreement with those from the Monte Carlo simulation [6], which are replotted as a line of circles in figure 3. It is emphasized that the formula for $\chi_{\alpha\alpha}$ in the case of $\lambda = 0$ is different from that in the case of $\lambda \neq 0$, which can be explained as the formation of two differently magnetic phases. Therefore, the role that the single-site anisotropy plays is similar to the one that inter-layer coupling plays; the latter case has been investigated by Singh and Elstner [3].

Figure 4 shows the temperature dependence of the specific heat. In the case of small λ the peak of the specific heat appears near $T \sim J_{ab}$ which is close to the Curie temperature $T_c \approx S(S+1)J_{ab}/3$, and shifts to the high-temperature side with increasing single-site anisotropy λ. The single-peak structure of the specific heat demonstrates that there exists one phase transition, with two phases formed. The specific heat data can be compared with those from the Monte Carlo simulation [6] which are replotted as a line of circles in this figure.

In conclusion, using a double-time Green's function we have investigated the Heisenberg antiferromagnet with single-site anisotropy on the fully frustrated multilayer triangular lattice. The critical value of the single-site anisotropy parameter is estimated at $\lambda \approx 0.2$. In the case of $\lambda < \lambda_c$ the spin-wave excitation is gapless; in the case of $\lambda > \lambda_c$ the spin-wave-excitation gap opens. We reason that the origin of the spin gap is closely related to the magnetic anisotropy. The axial susceptibility shows a clear peak near $T \sim J_{ab}$, but the planar one behaves quite differently. This anisotropic behaviour of the two susceptibilities is due to the appearance of the single-site anisotropy. The specific heat shows a clear peak near $T \sim J_{ab}$ and indicates that there exists one phase transition.

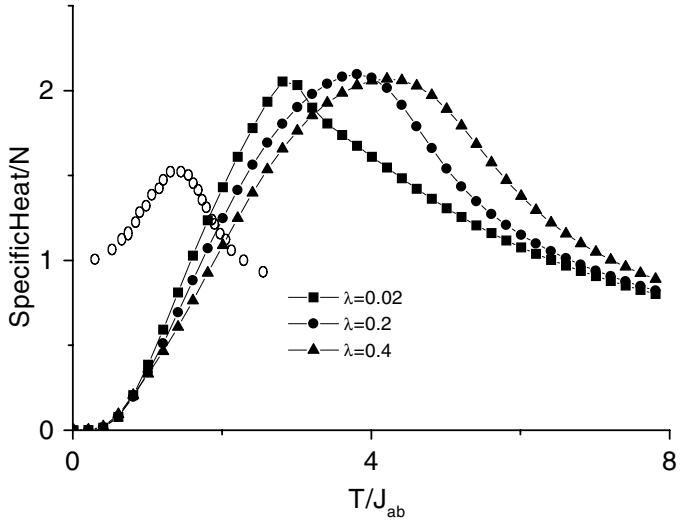

Figure 4. The specific heat against the reduced temperature T/J_{ab}. The line of circles represents the Monte Carlo simulation result taken from reference [6].

Acknowledgments

The authors would like to thank Qin Wang for useful discussion. This work was supported by the National Natural Science Foundation through Grant No 19774040.

References

[1] Sachdev S 1992 *Phys. Rev.* B **45** 12 377 and references therein
[2] Leung P W and Runge K J 1993 *Phys. Rev.* B **47** 5861
[3] Singh R R P and Elstner N 1998 *Phys. Rev. Lett.* **23** 4732
[4] Kawamura H 1998 *J. Phys.: Condens. Matter* **10** 4707
[5] Dong Zhanhai and Wang Yuqing 1997 *J. Phys.: Condens. Matter* **9** 10 457
[6] Todate Y, Himoto E, Kikuta C, Tanaka M and Suzuki J 1998 *Phys. Rev.* B **57** 485
[7] Ono T, Tanaka H, Kato T and Iio K 1998 *J. Phys.: Condens. Matter* **10** 7209
[8] Kondo J and Yamaji K 1972 *Prog. Theor. Phys.* **47** 807
[9] Kampf A P 1994 *Phys. Rep.* **249** 219 and references therein
[10] Sokol A and Pines D 1993 *Phys. Rev. Lett.* **71** 2813